8-30-2022

Truncated Matrix Power Iteration for Differentiable DAG Learning

Zhen Zhang

Ignavier Ng

Dong Gong

Yuhang Liu

Ehsan M. Abbasnejad

See next page for additional authors

Authors

Zhen Zhang, Ignavier Ng, Dong Gong, Yuhang Liu, Ehsan M. Abbasnejad, Mingming Gong, Kun Zhang, and Javen Qinfeng Shi

Truncated Matrix Power Iteration for Differentiable DAG Learning

Zhen Zhang[*,1], **Ignavier Ng**[*,2], **Dong Gong**[3], **Yuhang Liu**[1], **Ehsan M Abbasnejad**[1], **Mingming Gong**[4], **Kun Zhang**[2,5], and **Javen Qinfeng Shi**[1]

[1]*The University of Adelaide* [2]*Carnegie Mellon University*
[3]*The University of New South Wales* [4]*The University of Melbourne*
[5]*Mohamed bin Zayed University of Artificial Intelligence*
{zhen.zhang02,yuhang.liu01,ehsan.abbasnejad,javen.shi}@adelaide.edu.au
{ignaviern g,kunz1}@cmu.edu dong.gong@unsw.edu.au mingming.gong@unimelb.edu.au

Abstract

Recovering underlying Directed Acyclic Graph structures (DAG) from observational data is highly challenging due to the combinatorial nature of the DAG-constrained optimization problem. Recently, DAG learning has been cast as a continuous optimization problem by characterizing the DAG constraint as a smooth equality one, generally based on polynomials over adjacency matrices. Existing methods place very small coefficients on high-order polynomial terms for stabilization, since they argue that large coefficients on the higher-order terms are harmful due to numeric exploding. On the contrary, we discover that large coefficients on higher-order terms are beneficial for DAG learning, when the spectral radiuses of the adjacency matrices are small, and that larger coefficients for higher order terms can approximate the DAG constraints much better than the small counterparts. Based on this, we propose a novel DAG learning method with efficient truncated matrix power iteration to approximate geometric series based DAG constraints. Empirically, our DAG learning method outperforms the previous state-of-the-arts in various settings, often by a factor of 3 or more in terms of structural Hamming distance.

1 Introduction

Recovery of Directed Acyclic Graphs (DAGs) from observational data is a classical problem in many fields, including bioinformatics [27, 43], machine learning [16], and causal inference [34]. The graphical model produced by a DAG learning algorithm allows one to decompose the joint distribution over the variables of interest in a compact and flexible manner, and under certain assumptions [24, 34], these graphical models can have causal interpretations.

DAG learning methods can be roughly categorized into constraint-based and score-based methods. Most constraint-based approaches, e.g., PC [32], FCI [10, 33], rely on conditional independence test and thus may require a large sample size [29, 37]. The score-based approaches, including exact methods based on dynamic programming [15, 30, 31], A* search [41, 42], and integer programming [12], as well as greedy methods like GES [8], model the validity of a graph according to some score function and are often formulated and solved as a discrete optimization problem. A key challenge for score-based methods is the combinatorial search space of DAGs [7, 9].

[*]Equal Contribution

Preprint. Under review.

There is a recent interest in developing continuous optimization methods for DAG learning in the past few years. In particular, Zheng et al. [44] develops an algebraic characterization of DAG constraint based on a continuous function, specifically matrix exponential, of the weighted adjacency matrix of a graph, and applies it to estimate linear DAGs with equal noise variances using continuous constrained optimization [3, 4]. The resulting algorithm is called NOTEARS. Yu et al. [39] proposes an alternative DAG constraint based on powers of a binomial to improve practical convenience. Wei et al. [38] unifies these two DAG constraints by writing them in terms of a general polynomial one. These DAG constraints have been applied to more complex settings, e.g., with nonlinear relationships [17, 22, 39, 45], time series [23], and confounders [5], and have been shown to produce competitive performance. Apart from the polynomial based constraints, Lee et al. [18], Zhu et al. [46] present alternative formulations of the DAG constraints based on the spectral radius of the weighted adjacency matrix. Instead of solving a constrained optimization problem, Yu et al. [40] proposes NOCURL which employs an algebraic representation of DAGs such that continuous unconstrained optimization can be carried out in the DAG space directly. However, the focus of these works [18, 40, 46] is to improve the scalability, and the performance of the resulting methods may degrade.

To avoid potential numerical exploding that may be caused by high-order terms in the polynomial-based DAG constraints, previous works use very small coefficients for high terms in DAG constraints [39, 44]. More precisely, the coefficients decrease quickly to very small values for the relatively higher order terms that are still crucial for capturing the useful higher-order information. This causes difficulties for the DAG constraints to capture the higher order information for enforcing acyclicity. With such DAG constraints, a possible solution to maintain higher-order information for acyclicity is to apply an even larger penalty weight [39, 44], which, however, causes an ill-conditioning issue as shown in [21]. Moreover, these small coefficients will also be multiplied on the gradients of higher-order terms, leading to gradient vanishing. In this paper, we show that, on the contrary, larger coefficients may be safely used to construct more informative higher-order terms without introducing numeric exploding. The reason is that the weighted adjacency matrix of a DAG must be nilpotent; thus the candidate adjacency matrix often has a very small spectral radius. As a result, the higher order power of the matrix is very close to zero matrix, and larger coefficients may be safely used without causing numeric exploding. We thus propose to use geometric series-based DAG constraint without small coefficients for more accurate and robust DAG learning. To relieve the computational burden from the geometric series, we propose an efficient Truncated Matrix Power Iteration (TMPI) algorithm with a theoretically guaranteed error bound. We summarize our contributions as the following:

- We demonstrate that the key challenge for DAG learning is the gradient vanishing issue instead of gradient and numeric exploding. For sparse graphs, the gradient vanishing issue can be severe.
- We design a DAG constraint based on finite geometric series which is an order-d polynomial over adjacency matrices to escape from gradient vanishing. We show that the relatively large coefficients on the higher order terms would not result in gradient exploding in practice.
- We show that there exists some constant $k \leqslant d$, *s.t.* our order-d polynomial constraint can be reduced to order-k polynomial without expanding its feasible set. Though finding such value of k requires solving the NP-hard longest simple path problem, we develop a simple heuristic to find such k with bounded error to the exact, order-d, DAG constraint. Based on this result, we propose a DAG constraint based on efficient Truncated Matrix Power Iteration (TMPI), and conduct experiments to demonstrate that the resulting DAG learning method outperforms previous methods by a large margin.
- We provide a systematical empirical comparison of the existing DAG constraints, including the polynomial and spectral radius based constraints, as well as the algebraic DAG representation of NOCURL.

2 Preliminaries

DAG Model and Linear SEM Given a DAG model (a.k.a. Bayesian network) defined over random vector $\mathbf{x} = [x_1, x_2, \ldots, x_d]^\top$ and DAG $\mathcal{G}$, the distribution $P(\mathbf{x})$ and DAG $\mathcal{G}$ are assumed to satisfy the Markov assumption [24, 34]. We say that $\mathbf{x}$ follows a linear Structural Equation Model (SEM) if

$$\mathbf{x} = \mathbf{B}^\top \mathbf{x} + \mathbf{e}, \tag{1}$$

where $\mathbf{B}$ is the weighted adjacency matrix representing the DAG $\mathcal{G}$, and $\mathbf{e} = [e_1, e_2, \ldots, e_d]^\top$ denotes the exogenous noise vector consisting of d independent random variables. With slight abuse of notation, we denote by $\mathcal{G}(\mathbf{B})$ the graph induced by weighted adjacency matrix $\mathbf{B}$. Moreover, we do not distinguish between random variables and vertices or nodes, and use these terms interchangeably.

Our goal is to estimate the DAG $\mathcal{G}$ from n i.i.d. examples of $\mathbf{x}$, indicated by the matrix $\mathbf{X} \in \mathbb{R}^{n \times d}$. In general, the DAG $\mathcal{G}$ can only be identified up to its Markov equivalence class under the faithfulness [34] or sparsest Markov representation [26] assumption. It has been shown that for linear SEMs with homoscedastic errors, from which the noise terms are specified up to a constant [19], and for linear non-Gaussian SEMs, from which no more than one of the noise term is Gaussian, the true DAG can be fully identified. In this work, we focus on the linear SEMs with equal noise variances [25], which can be viewed as an instance of the former.

DAG Constraints for Differentiable Structure Learning Recently, Zheng et al. [44] reformulated the DAG learning problem as the following continuous optimization problem with convex least-squares objective but non-convex constraint,

$$\min_{\mathbf{B} \in \mathbb{R}^{d \times d}} \quad \| \mathbf{X} - \mathbf{X}\,\mathbf{B} \|_F^2 + \eta \| \mathbf{B} \|_1, \quad \text{subject to } h_{\text{exp}}(\mathbf{B} \odot \mathbf{B}) = 0, \tag{2}$$

where $\| \cdot \|_F$ and $\| \cdot \|_1$ denote the Frobenius norm and elementwise ℓ_1 norm, respectively, $\eta > 0$ is the regularization coefficient that controls the sparsity of $\mathbf{B}$, and $\odot$ denotes the Hadamard product, which is used to map $\mathbf{B}$ to a positive weighted adjacency matrix with the same structure. Given any $\tilde{\mathbf{B}} \in \mathbb{R}^{d \times d}_{\geqslant 0}$, the function h_{exp} is defined as

$$h_{\text{exp}}(\tilde{\mathbf{B}}) = \operatorname{tr}(e^{\tilde{\mathbf{B}}}) - d = \operatorname{tr}\left(\sum_{i=1}^{\infty} \frac{1}{i!} \tilde{\mathbf{B}}^i \right), \tag{3}$$

and can be efficiently computed using various different approaches [1, 2]. The formulation (2) involves a hard constraint, which is solved using the augmented Lagrangian method [3, 4] specifically developed for constrained optimization.

To improve practical convenience, Yu et al. [39] proposed a similar DAG constraint using an order-d polynomial based on powers of a binomial, given by

$$h_{\text{bin}}(\tilde{\mathbf{B}}) = \operatorname{tr}\left(\mathbb{I} + \alpha \tilde{\mathbf{B}} \right)^d - d = \operatorname{tr}\left(\sum_{i=1}^{d} \binom{d}{i} \alpha^i \tilde{\mathbf{B}}^i \right), \tag{4}$$

where $\alpha > 0$ is a hyperparameter and is often set to $1/d$, e.g., in the implementation of DAG-GNN [39]. This function can be evaluated using $O(\log d)$ matrix multiplications using the exponentiation by squaring algorithm. Both $h_{\text{exp}}(\tilde{\mathbf{B}})$ and $h_{\text{bin}}(\tilde{\mathbf{B}})$ are formulated by [38] as a unified one

$$h_{\text{poly}}(\tilde{\mathbf{B}}) = \operatorname{tr}\left(\sum_{i=1}^{d} c_i \tilde{\mathbf{B}}^i \right), \quad c_i > 0, \quad i = 1, 2, \ldots, d. \tag{5}$$

3 DAG Learning using Truncated Matrix Power Iteration

In this section, we first show that gradient vanishing is one main issue for previous DAG constraints and propose a truncated geometric series based DAG constraints to escape from the issue in Section 3.1. Then in Section 3.2 the theoretic properties of our DAG constraints are analyzed. In Section 3.3 we provide an efficient algorithm for our DAG constraints. In Section 3.4, we discuss the relation between our algorithm and previous works.

3.1 Truncated Geometric DAG Constraints

Theoretically, any positive values of c_i suffice to make the DAG constraint term $h_{\text{poly}}(\tilde{\mathbf{B}})$ in Eq. (5) a valid one, i.e., it equals zero if and only if the graph $\mathcal{G}(\tilde{\mathbf{B}})$ is acyclic. Thus previously small coefficients for higher order terms are preferred since they are known to have better resistance to numerical exploding of higher order polynomials [39, 44]. These small coefficients forbid informative

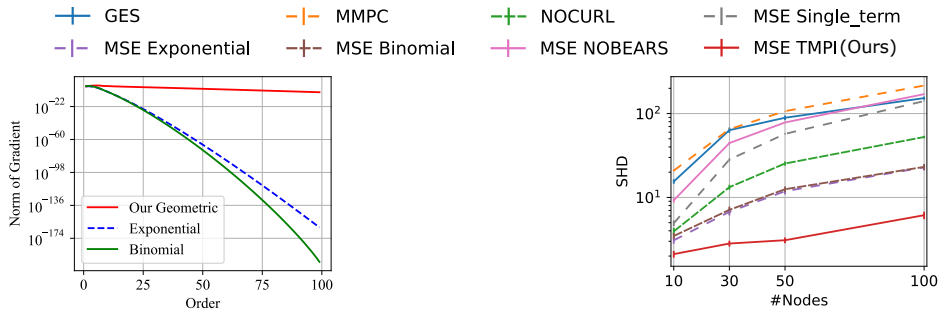

Figure 1: Previous polynomial based DAG constraints, including exponential (Eq. (3)) and binomial (Eq. (4) with $\alpha = 1/d$) constraints, suffers from gradient vanishing. **Left** show the norm of gradient on higher order terms w.r.t. order on a 100-node graph. We proposed a geometric series based DAG constraints, named Truncated Matrix Power Iteration (TMPI) to escape from vanished gradients and it leads to a significant performance improvement in terms of Structural Hamming Distance (SHD) on ER3 graphs shown in the **Right**(we refer to Section 4 for more details.). Note that the gradients on different order terms refer to $\nabla_{\tilde{\mathbf{B}}} c_i \operatorname{tr}(\tilde{\mathbf{B}}^i)$, where, for different polynomial based DAG constraints, the coefficients c_i are different.

higher order terms and cause severe gradient vanishing, as nilpotent properties of DAG result in candidate adjacency matrix with very small spectral radius (see empirical results in Figure 1 Left). In this case, the weight updates during the optimization process can hardly utilize this higher-order information from the vanishingly small gradients. As a consequence, only lower-order information can be effectively captured, which may be detrimental to the quality of learned DAG.

To avoid the severe vanishing gradient issue in previous DAG constraint (*e.g.*, Eq. (3), (4)), we propose to discard the coefficients and use a finite geometric series based function:

$$h_{\text{geo}}(\tilde{\mathbf{B}}) = \operatorname{tr}\left(\sum_{i=1}^{d} \tilde{\mathbf{B}}^i\right), \qquad (6) \qquad \nabla_{\tilde{\mathbf{B}}} h_{\text{geo}}(\tilde{\mathbf{B}}) = \left[\sum_{i=0}^{d-1} (i+1)\tilde{\mathbf{B}}^i\right]^\top. \qquad (7)$$

The gradient of h_{geo} w.r.t. $\tilde{\mathbf{B}}$ denoted by $\nabla_{\tilde{\mathbf{B}}} h_{\text{geo}}(\tilde{\mathbf{B}})$ is to an order-$(d-1)$ polynomial of $\tilde{\mathbf{B}}$.

With the same d, Eq. (6) is a more precise DAG constraint escaped from from severe gradient vanishing. Also it is notable that due to the nilpotent properties of weighted adjacency matrices of DAGs, the higher order terms in (6) and (7) often comes with small norms and thus our DAG constraint would not suffer from numerical exploding.

In Figure 1 we compared the norm of gradients on higher order terms of different DAG constraints, where we can see that for previous exponential-based (3) and binomial-based (4) DAG constraints, the gradients of higher order terms converges to 0 very quickly as order increases. Meanwhile, the gradient of higher order terms in (6) converges to 0 with a much slower speed and thus informative higher order terms are reserved.

We further show that those non-informative higher-order terms that are close to zero in (6) can be safely dropped to form a more efficient DAG constraint with some $k \ll d$:

$$h^k_{\text{trunc}}(\tilde{\mathbf{B}}) = \operatorname{tr}\left(\sum_{i=1}^{k} \tilde{\mathbf{B}}^i\right). \qquad (8)$$

The DAG constraints (8) requires $\mathcal{O}(k)$ matrix multiplication which is far less than $\mathcal{O}(d)$ for (6), and under quite mild conditions the error of (8) is tightly bounded (See Proposition 3 for details). In Figure 1 **right** we show that our DAG constraint (8) (named TMPI) attains far better performance than previous ones as it escapes from gradient vanishing.

3.2 Theoretic Properties for Truncated Geometric DAG Constraint

We analyze the properties of the power of adjacency matrices, which play an important role in constructing DAG constraints. First notice that, for the k^{th} power of an adjacency matrix $\tilde{\mathbf{B}} \in \mathbb{R}^{d\times d}_{\geqslant 0}$, its entry $(\tilde{\mathbf{B}}^k)_{ij}$ is nonzero if and only if there is a length-k path (not necessarily simple) from node X_i to node X_j in graph $\mathcal{G}(\tilde{\mathbf{B}})$. This straightforwardly leads to the following property, which is a corollary of [38, Lemma 1].

Proposition 1. *Let $\tilde{\mathbf{B}} \in \mathbb{R}_{\geqslant 0}^{d\times d}$ be the weighted adjacency matrix of a graph $\mathcal{G}$ with d vertices. $\mathcal{G}$ is a DAG if and only if $\tilde{\mathbf{B}}^d = \mathbf{0}$.*

Proposition 1 can be used to construct a single-term DAG constraint term, given by

$$h_{\text{single}}(\tilde{\mathbf{B}}) = \|\tilde{\mathbf{B}}^d\|_p, \tag{9}$$

where $\|\cdot\|_p$ denotes an elementwise ℓ_p norm. However, as the candidate adjacency matrix gets closer to acyclic, the spectral radius of $\tilde{\mathbf{B}}^d$ will become very small. As a result, the value $h_{\text{single}}(\tilde{\mathbf{B}})$, as well as its gradient $\nabla_{\tilde{\mathbf{B}}} h_{\text{single}}(\tilde{\mathbf{B}})$ may become too small to be represented in limited machine precision. This suggests the use of the polynomial based constraints for better performance.

Without any prior information of the graph, one has to compute the d^{th} power of matrix $\tilde{\mathbf{B}}$, either using the DAG constraint terms in Eq. (9) or (5). However, if the length of the longest simple path in the graph is known, we can formulate a lower order polynomial based DAG constraint.

Proposition 2. *Let $\tilde{\mathbf{B}} \in \mathbb{R}_{\geqslant 0}^{d\times d}$ be the weighted adjacency matrix of a graph $\mathcal{G}$ with d vertices, and k be the length of the longest simple path[1] in graph $\mathcal{G}$. The following three conditions are equivalent: (1) $\mathcal{G}$ is a DAG, (2) $\tilde{\mathbf{B}}^{k+1} = 0$, and (3) $h^k_{trunc}(\tilde{\mathbf{B}}) = 0$.*

The intuition of the above proposition is as follows. For the graph whose largest cycle has a length of k, it suffices to compute the k^{th} power of its adjacency matrix, since computing any power larger than k is simply traveling in the cycles repeatedly. Therefore, Proposition 2 suggests that $h^k_{\text{trunc}}(\tilde{\mathbf{B}}) = 0$ is a valid DAG constraint.

Unfortunately, the longest simple path problem for general graphs is known to be NP-hard [28], and thus we have to find an alternative way to seek the proper k. For a candidate adjacency matrix $\mathbf{B}$, a simple heuristic is to iterate over the power of matrices to find some k *s.t.* matrix $\tilde{\mathbf{B}}^k$ is close enough to a zero matrix. Recall that Proposition 1 implies that the adjacency matrix of a DAG is nilpotent; therefore, when a candidate adjacency matrix $\tilde{\mathbf{B}}$ is close to being acyclic, its spectral radius would be close to zero, which means that the $\tilde{\mathbf{B}}^k$ would converge quickly to zero as k increases. Thus, if we use the above heuristic to find k, it is highly possible we find some $k \ll d$.

By using an approximate k instead of the exact one, the DAG constraints in Eq. (8) becomes an approximate one with the following bounds. Denoting by $\|\cdot\|_\infty$ the element-wise infinity norm (i.e., maximum norm), we have the following proposition.

Proposition 3. *Given $\tilde{\mathbf{B}} \in \mathbb{R}_{\geqslant 0}^{d\times d}$, if there exists $k < d$ such that $\|\tilde{\mathbf{B}}^k\|_\infty \leqslant \epsilon < \frac{1}{(k+1)d}$, then we have*

$$0 \leqslant h_{geo}(\tilde{\mathbf{B}}) - h^k_{trunc}(\tilde{\mathbf{B}}) \leqslant d^{2+1/k} \cdot \frac{1-(d\epsilon)^{d/k-1}}{1-(d\epsilon)^{1/k}} \epsilon^{1+1/k}, \quad \textit{and}$$
$$0 \leqslant \|\nabla_{\tilde{\mathbf{B}}} h_{geo}(\tilde{\mathbf{B}}) - \nabla_{\tilde{\mathbf{B}}} h^k_{trunc}(\tilde{\mathbf{B}})\|_F \leqslant (k+1)d\epsilon \|\nabla_{\tilde{\mathbf{B}}} h_{geo}(\tilde{\mathbf{B}})\|_F.$$

Remark 1. *The bound $\epsilon < \frac{1}{(k+1)d}$ is needed in the proposition above such that the inequalities are non-vacuous, specifically since we must have $\|\nabla_{\tilde{\mathbf{B}}} h_{geo}(\tilde{\mathbf{B}}) - \nabla_{\tilde{\mathbf{B}}} h^k_{trunc}(\tilde{\mathbf{B}})\|_F / \|\nabla_{\tilde{\mathbf{B}}} h_{geo}(\tilde{\mathbf{B}})\|_F < 1$.*

Proposition 3 provides an efficient way to bound the error of truncated constraints $h^k_{\text{trunc}}(\tilde{\mathbf{B}})$ to the geometric series based DAG constraints $h_{\text{geo}}(\tilde{\mathbf{B}})$. However, it also demonstrates a possible limitation for all polynomial based DAG constraints. As we know, when a solution is close to DAG, its spectral radius must be close to zero. In this situation, if the longest simple path in a graph is very long, it is unavoidable to use very high order terms to capture this information while such higher order might be very close to 0. In the worst case, the higher terms may be underflow due to limited machine precision. Thus some specific numerically stable method may be required, and we leave this for future work.

[1] We use simple path to refer to a path that repeats no vertex, except that the first and last may be the same vertex [14, p. 363].

3.3 Dynamic Truncated Matrix Power Iteration

From Proposition 3, we know that it would be safe to ignore those matrix powers with index larger than k. The DAG constraint and its gradient, become order-k polynomials of $\mathbf{B}$. A straightforward way to compute the DAG constraint as well as the gradient is provided in Algorithm 1, which we call TMPI. For general polynomial based DAG constraints in (5), it requires $\mathcal{O}(d)$ times matrix multiplication, and our Algorithm 1 can reduce the number of multiplication to $\mathcal{O}(k)$ (in practice k is much smaller than d). For example, when recovering 100-node Erdős–Rényi DAG with expected degree 4, k is often smaller than 20.

Fast Truncated Matrix Power Iteration The specific structure of geometric series can be used to further accelerate the TMPI algorithm from $\mathcal{O}(k)$ to $\mathcal{O}(\log k)$ matrix multiplications, based on the following results (the proof is provided in Appendix A.5).

Proposition 4. *Given any $d\times d$ real matrix $\tilde{\mathbf{B}}$, let $f_i(\tilde{\mathbf{B}}) = \tilde{\mathbf{B}}+\tilde{\mathbf{B}}^2+\cdots+\tilde{\mathbf{B}}^i$ and $h_i(\tilde{\mathbf{B}}) = \operatorname{tr}(f_i(\tilde{\mathbf{B}}))$, we have the following recurrence relations:*

$$\begin{aligned} f_{i+j}(\tilde{\mathbf{B}}) =& f_i(\tilde{\mathbf{B}}) + \tilde{\mathbf{B}}^i f_j(\tilde{\mathbf{B}}), \\ \nabla_{\tilde{\mathbf{B}}} h_{i+j}(\tilde{\mathbf{B}}) =& \nabla_{\tilde{\mathbf{B}}} h_i(\tilde{\mathbf{B}}) + (\tilde{\mathbf{B}}^i)^\top \nabla_{\tilde{\mathbf{B}}} h_j(\tilde{\mathbf{B}}) + i f_j(\tilde{\mathbf{B}})^\top (\tilde{\mathbf{B}}^{i-1})^\top. \end{aligned}$$

It is straightfoward to obtain the following corollary by setting $i = j$ in Proposition 4.

Corollary 1. *Given any matrix $d \times d$ real matrix $\tilde{\mathbf{B}}$, let $f_i(\tilde{\mathbf{B}}) = \tilde{\mathbf{B}} + \tilde{\mathbf{B}}^2 + \cdots + \tilde{\mathbf{B}}^i$ and $h_i(\tilde{\mathbf{B}}) = \operatorname{tr}(f_i(\tilde{\mathbf{B}}))$, we have have the following recurrence relations:*

$$\begin{aligned} f_{2i}(\tilde{\mathbf{B}}) =& f_i(\tilde{\mathbf{B}}) + \tilde{\mathbf{B}}^i f_i(\tilde{\mathbf{B}}), \\ \nabla_{\tilde{\mathbf{B}}} h_{2i}(\tilde{\mathbf{B}}) =& \nabla_{\tilde{\mathbf{B}}} h_i(\tilde{\mathbf{B}}) + (\tilde{\mathbf{B}}^i)^\top \nabla_{\tilde{\mathbf{B}}} h_i(\tilde{\mathbf{B}}) + i \left[f_{2i}(\tilde{\mathbf{B}}) - f_i(\tilde{\mathbf{B}}) + \tilde{\mathbf{B}}^i - \tilde{\mathbf{B}}^{2i} \right]^\top. \end{aligned}$$

This suggests that instead of increasing the index i (referring to the power of $\tilde{\mathbf{B}}$), arithmetically by 1, as in line 9 of Algorithm 1, we can use the recurrence relations in Corollary 1 to increase the index i geometrically by a factor of 2, until the condition $\|\tilde{\mathbf{B}}^i\|_\infty \leqslant \epsilon$ is satisfied. The full procedure named Fast TMPI is available in Algorithm 2, which requires $\mathcal{O}(\log k)$ matrix multiplications and $\mathcal{O}(d^2)$ additional storage. Similar strategy can be applied to the original geometric series based constraint (6) to form a fast algorithm that requires $\mathcal{O}(\log d)$ matrix multiplications.

Algorithm 1 Truncated Matrix Power Iteration (TMPI)

Input $\tilde{\mathbf{B}} \in \mathbb{R}_{\geqslant 0}^{d\times d}$, ϵ
Output $h(\tilde{\mathbf{B}}), \nabla_{\tilde{\mathbf{B}}} h(\tilde{\mathbf{B}})$

1: $i \leftarrow 2, h(\tilde{\mathbf{B}}) \leftarrow \operatorname{tr}(\tilde{\mathbf{B}}), \nabla_{\tilde{\mathbf{B}}} h(\tilde{\mathbf{B}}) \leftarrow \mathbb{I}$
2: **while** $i \leqslant d$ **do**
3: $\quad \nabla_{\tilde{\mathbf{B}}} h(\tilde{\mathbf{B}}) \leftarrow \nabla_{\tilde{\mathbf{B}}} h(\tilde{\mathbf{B}}) + i(\tilde{\mathbf{B}}^{i-1})^\top$
4: $\quad \tilde{\mathbf{B}}^i \leftarrow \tilde{\mathbf{B}}\tilde{\mathbf{B}}^{i-1}$
5: $\quad h(\tilde{\mathbf{B}}) \leftarrow h(\tilde{\mathbf{B}}) + \operatorname{tr}(\tilde{\mathbf{B}}^i)$
6: $\quad$ **if** $\|\tilde{\mathbf{B}}^i\|_\infty \leqslant \epsilon$ **then**
7: $\quad\quad$ **break**
8: $\quad$ **end if**
9: $\quad i \leftarrow i + 1$
10: **end while**
11: **Output** $h(\tilde{\mathbf{B}}), \nabla_{\tilde{\mathbf{B}}} h(\tilde{\mathbf{B}})$

Algorithm 2 Fast TMPI

Input $\tilde{\mathbf{B}} \in \mathbb{R}_{\geqslant 0}^{d\times d}$, ϵ
Output $h(\tilde{\mathbf{B}}), \nabla h(\tilde{\mathbf{B}})$

1: $i \leftarrow 1$
2: $\tilde{\mathbf{B}}_f \leftarrow \tilde{\mathbf{B}}, \tilde{\mathbf{B}}_g \leftarrow \mathbb{I}, \tilde{\mathbf{B}}_p \leftarrow \tilde{\mathbf{B}}$ {$\tilde{\mathbf{B}}_f$ stores f_i, $\tilde{\mathbf{B}}_f$ stores $\nabla \operatorname{tr} f_i$, and $\tilde{\mathbf{B}}_p$ stores $\tilde{\mathbf{B}}^i$}
3: **while** $i \leqslant d$ **do**
4: $\quad \tilde{\mathbf{B}}_f^{old} \leftarrow \tilde{\mathbf{B}}_f, \tilde{\mathbf{B}}_g^{old} \leftarrow \tilde{\mathbf{B}}_g, \tilde{\mathbf{B}}_p^{old} \leftarrow \tilde{\mathbf{B}}_p$
5: $\quad \tilde{\mathbf{B}}_f \leftarrow \tilde{\mathbf{B}}_f^{old} + \tilde{\mathbf{B}}_p^{old} \times \tilde{\mathbf{B}}_f^{old}, \tilde{\mathbf{B}}_p \leftarrow \tilde{\mathbf{B}}_p^{old} \times \tilde{\mathbf{B}}_p^{old}$
6: $\quad \tilde{\mathbf{B}}_g \leftarrow \tilde{\mathbf{B}}_g^{old} + \tilde{\mathbf{B}}_p^\top \tilde{\mathbf{B}}_g^{old} + i(\tilde{\mathbf{B}}_f - \tilde{\mathbf{B}}_f^{old} + \tilde{\mathbf{B}}_p^{old} - \tilde{\mathbf{B}}_p)$
7: $\quad$ **if** $\|\tilde{\mathbf{B}}_p\|_\infty \leqslant \epsilon$ **break**
8: $\quad i \leftarrow 2i$
9: **end while**
10: **Output** $\operatorname{tr}\left[\tilde{\mathbf{B}}_f\right], \tilde{\mathbf{B}}_g$

The Full Optimization Framework For NOTEARS, we apply the same augmented Lagrangian framework [3, 4] as Zheng et al. [44] to convert the constrained optimization problem into the following unconstrained problem

$$\min_{\mathbf{B}\in\mathbb{R}^{d\times d}} \ \| \mathbf{X} - \mathbf{X}\,\mathbf{B} \|_F^2 + \eta \| \mathbf{B} \|_1 + \frac{\rho}{2} h_{\text{trunc}}^k(\mathbf{B}\odot\mathbf{B})^2 + \alpha h_{\text{trunc}}^k(\mathbf{B}\odot\mathbf{B}), \tag{10}$$

where the parameters ρ and α are iteratively updated using the same strategy as Zheng et al. [44]. We also apply the proposed DAG constraint to GOLEM [20] that adopts likelihood-based objective with soft constraints, leading to the unconstrained optimization problem

$$\min_{\mathbf{B}\in\mathbb{R}^{d\times d}} \frac{d}{2}\log\|\mathbf{X}-\mathbf{X}\mathbf{B}\|_F^2 - \log|\det(\mathbb{I}-\mathbf{B})| + \eta_1\|\mathbf{B}\|_1 + \eta_2 h^k_{\text{trunc}}(\mathbf{B}\odot\mathbf{B}), \tag{11}$$

where $\eta_1, \eta_2 > 0$ are the regularization coefficients. In both formulations above, the value of k is dynamically computed and updated during each optimization iteration based on Algorithm 1 or 2.

3.4 Relation to Previous Works

Our algorithm is closely related to the following DAG constraint considered by Zheng et al. [44].

Lemma 1 (Zheng et al. [44, Proposition 1])**.** *Let $\tilde{\mathbf{B}} \in \mathbb{R}^{d\times d}_{\geqslant 0}$ with spectral radius small than one be the weighted adjacency matrix of a graph $\mathcal{G}$ with d vertices. $\mathcal{G}$ is a DAG if and only if*

$$\operatorname{tr}(\mathbb{I}-\tilde{\mathbf{B}})^{-1} = d. \tag{12}$$

The inverse of $\mathbb{I}-\tilde{\mathbf{B}}$ is just the geometric series as follows,

$$(\mathbb{I}-\tilde{\mathbf{B}})^{-1} = \sum_{i=0}^{\infty}\tilde{\mathbf{B}}^i. \tag{13}$$

Zheng et al. [44] argue that (13) is not well defined for $\tilde{\mathbf{B}}$ with spectral radius larger than 1, and in practice the series (13) may explode very quickly Based on this argument, they choose to use the matrix exponential to construct the DAG constraints. For the same reason Yu et al. [39] also use very small coefficients for higher terms in polynomial based DAG constraints. However, as we show in Section 3, Yu et al. [39], Zheng et al. [44] actually suffers more from gradient vanishing due to small coefficients for higher terms. In fact, our constraints (8) provide a good approximate for (12) since we are actually looking for an approximate inverse of $\mathbb{I}-\tilde{\mathbf{B}}$ with a bounded error.

Proposition 5. *Given $\tilde{\mathbf{B}} \in \mathbb{R}^{d\times d}_{\geqslant 0}$, if for some k, $\|\tilde{\mathbf{B}}^k\|_\infty \leqslant \epsilon < 1/d$, then*

$$\left\|(\mathbb{I}-\tilde{\mathbf{B}})^{-1} - \sum_{i=0}^{k}\tilde{\mathbf{B}}^k\right\|_F \leqslant d\epsilon\left\|(\mathbb{I}-\tilde{\mathbf{B}})^{-1}\right\|_F.$$

Previous works [21, 38] pointed out that for constraints with form $h(\mathbf{B}\odot\mathbf{B})$, the Hadamard product would lead to vanishing gradients since $\nabla_{\mathbf{B}}h(\mathbf{B}\odot\mathbf{B}) = 0$ if and only if $h(\mathbf{B}\odot\mathbf{B}) = 0$. Therefore, this may lead to ill-conditioning issue [21]. One may replace the Hadamard product with absolute value, as in Wei et al. [38], but the non-smoothness of absolute value makes the optimization problem difficult to solve and may lead to poorer performance [21]. As pointed out by Ng et al. [21], Quasi-Newtown methods, e.g., L-BFGS [6], still perform well even when faced with the ill-conditioning issue caused by vanishing gradients of constraints with form $h(\mathbf{B}\odot\mathbf{B})$. In this work, we identify another type of gradient vanishing issue caused by (1) the higher order terms and small coefficients in h itself and (2) the small spectral radius of candidate $\mathbf{B}$, and provide an effective solution by constructing a Truncated Matrix Power Iteration based DAG constraint.

4 Experiments

We compare the performance of different DAG learning algorithms and DAG constraints to demonstrate the effectiveness of the proposed Truncated Matrix Power Iteration (TMPI)-based DAG constraints. We give an outline of the experimental settings in this section, and more details including the parameter settings can be found in supplementary files [2].

4.1 DAG Learning

We first conduct experiments on synthetic datasets using similar settings as previous works [39, 40, 44]. In summary, random Erdös-Rényi graphs are generated with d nodes and kd expected edges (Denoted by ERk), and edge weights generated from uniform distribution over the union of two intervals

[2]The source code for conducting all the experiments will be disclosed after publication of the paper.

$[-2, -0.5] \cup [0.5, 2.0]$ are assigned to each edge to form a weighted adjacency matrix $\mathbf{B}$. Then n random samples are generated from model $\mathbf{x} = \mathbf{B}\,\mathbf{x} + \mathbf{e}$ to form an $n \times d$ data matrix $\mathbf{X}$, where the noise $\mathbf{e}$ are i.i.d. sampled from Gaussian, Exponential, or Gumbel distribution. In our experiments, we set $n = 1000$, and 4 different $d = 10, 30, 50, 100$ are considered. For each setting, we generate 100 different graphs to obtain an average performance.

Models and Baselines We consider DAG learning framework based on both Mean Square Error(MSE) loss (see Eq. (10)) and likelihood-based (see Eq. (11)) loss from GOLEM [20]. For both losses, we include the following DAG constraints: (1) MSE/Likelihood loss+Exponential DAG constraint (3), *i.e.* NOTEARS [44]/GOLEM[20] ; (2) MSE/Likelihood loss+Binomial DAG constraint (4) from DAG-GNN [39]; (3) MSE/Likelihood loss+Spectral radius based DAG constraint from NOBEARS [18]; (4) MSE/Likelihood loss+Single Term DAG constraint (9); (5) MSE/Likelihood loss+Truncated Matrix Power Iteration (TMPI) based DAG constraint (8). For the NOCURL [40] DAG constraint, since it is designed as a two stage methods where the initialization stage rely on MSE loss and Binomial DAG constraint, we include it as a baseline, but do not combine it with likelihood loss. The other baselines that we are comparing to including GES [8] and MMPC [36].

For MSE loss based DAG learning algorithms (10)), we set $\eta = 0.1$ and use the same search strategy as Zheng et al. [44] to update the parameters ρ and α. For likelihood loss based DAG learning algorithms (11), we set $\eta_1 = 0.02$ and $\eta_2 = 5.0$ as Ng et al. [20]. For the Binomial DAG constraints (4), the parameter α is set to $1/d$ as [39]. For our TMPI DAG constraint, we set the parameter $\epsilon = 10^{-6}$. For the NOCURL algorithm, we use their public available implementation and default parameter setting[3]. For GES and MMPC, we use the implementation and default parameter setting in Kalainathan and Goudet [13].

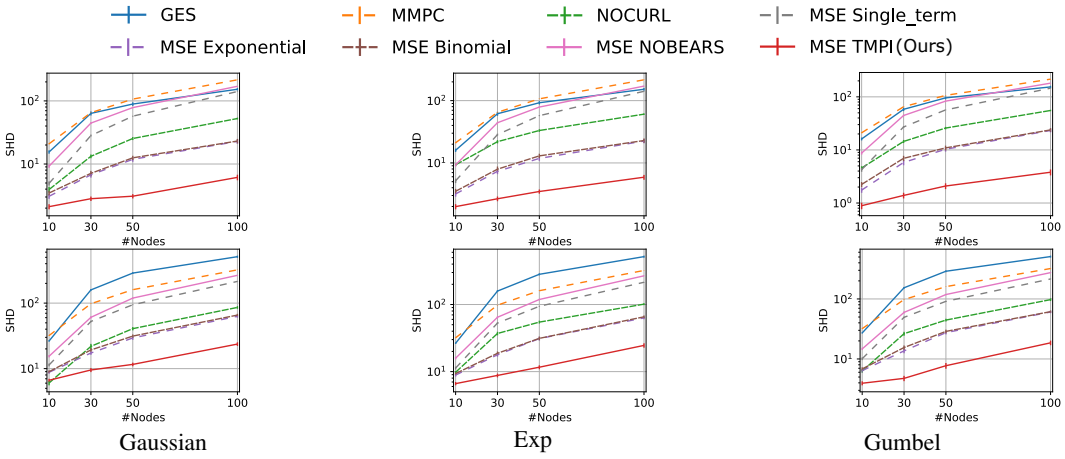

Figure 2: Structural discovery results of MSE loss (*e.g.* Eq. (10)) based algorithms and baselines in terms of SHD (lower is better) on ER2 (Top) and ER3 (Bottom) graphs, where our algorithm consistently outperforms others almost by **an order of magnitude**. Error bars represent standard errors over 100 simulations.

[3] `https://github.com/fishmoon1234/DAG-NoCurl/blob/master/main_efficient.py` from commit 4e2a1f4 on 14 Jun 2021. Better performance may be attained by tuning the hyper-parameters, but the current best reported performance is slightly worse than NOTEARS.

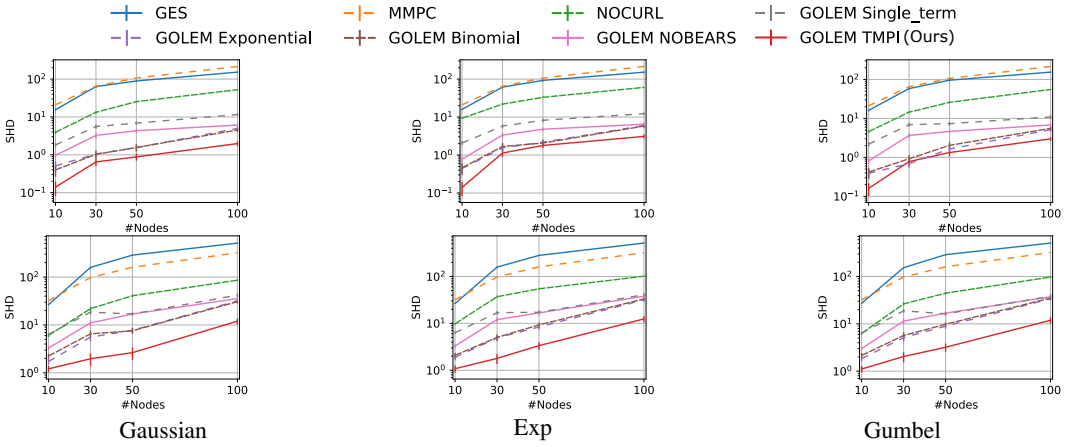

Figure 3: Structural discovery results of likelihood loss (*i.e.* Eq. (11)) based algorithms and baselines in terms of SHD (lower is better) on ER2 (top) and ER3 (bottom) graphs, where our algorithm consistently outperforms others in a large margin in almost all cases. Error bars represent standard errors over 100 simulations.

Results The result for MSE/likelihood based DAG learning algorithm is shown in Figure 2/3 , where we compared the Structural Hamming Distance (SHD) of different algorithms. The Original NOTEARS (*i.e.* MSE+Exponential) / GOLEM (*i.e.* GOLEM+Exponential) has similar performance as MSE/GOLEM+Binomial. This is as expected since the coefficients of each order in Exponential and Binomial constraints are actually very close (See Figure 1). The performance of algorithms using single-term loss is often not comparable to the other polynomial-based constraints since it suffers more from gradient vanishing. The performance of algorithms using the spectral radius based constraints (BEARS) are also worse than the ones using Exponential and Binomial constraints. The algorithms using our TMPI constraints outperforms all others in almost all cases, which demonstrates the effectiveness of our DAG constraint.

4.2 Extension to Nonlinear Case

Our algorithm are mainly designed for linear cases but it can be straightforwardly extended to nonlinear cases. In this section, we extend our DAG constraint to nonlinear case by replacing the binomial DAG constraint in DAG-GNN [39], NOTEARS-MLP[45] and GRAN-DAG[17] with ours.

Synthetic data We conducted an experiment to compare our algorithm and DAG-GNN on 50-node ER1 graph with nonlinear SEM $\mathbf{x} = \mathbf{B}\cos(\mathbf{x}+1) + \mathbf{e}$ over 5 simulations. Our algorithm achieves SHD of 22.2 ± 4.2 while DAG-GNN achieves SHD of 25.2 ± 4.5. We simulated a nonlinear dataset with 50-node ER1 graphs and each function being an MLP as Zheng et al. [45]. The original NOTEARS-MLP has SHD 16.9 ± 1.5, while NOTEARS-MLP with our TMPI constraint achieves an SHD of 14.9 ± 1.3.

Real Data We also run an experiment on the Protein Signaling Networks (PSN) dataset [27] consisting of $n = 7466$ samples with $d = 11$ nodes. The PSN dataset are widely used to evluate the performance of nonlinear DAG recovery algorithms, however since the identifiability of the DAG is not guaranteed we compare both SHD and SHDC (SHD of CPDAG) as [17]. In this experiments, we replace the original DAG constraints in DAG-GNN[39] and Gran-DAG[17] with our TMPI DAG constraints. The results is shown in Table 1, and we can see that by replacing the DAG constraint with our TMPI constraint there is a performance improvement on SHD and SHDC (SHD of CPDAG) for almost all cases.

4.3 Ablation Study

We use the ER3 dataset in previous section to conduct an ablation study to compare the performance of the geometric constraints (6) and our TMPI constraints (8), with both naive implementations and the fast implementations based on Proposition 4 and Corollary 1. The results are shown in Figure 4. The SHD between Geometric constraint and TMPI constraints in both the naive and fast implementations are similar, and our Fast TMPI algorithm runs significantly faster than the other three.

Table 1: Experimental Results on Sachs Dataset. Our TMPI DAG constraint consistently outperforms other DAG constraints.

	SHD	SHDC
DAG-GNN	16	21
DAG-GNN/TMPI (Ours)	16	17
Gran-DAG	13	11
Gran-DAG/TMPI (Ours)	**12**	**9**
Gran-DAG++	13	10
Gran-DAG++/TMPI (Ours)	**12**	**9**

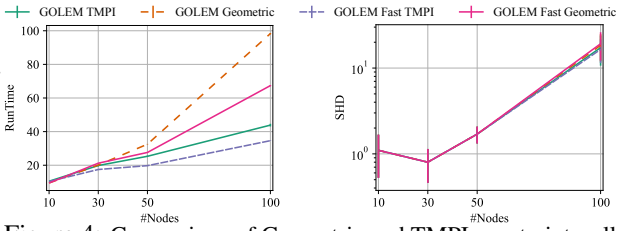

Figure 4: Comparison of Geometric and TMPI constraints, all algorithm achieves similar performance but our fast algorithm runs significantly faster. **Left:** Running time; **Right:** SHD. Error bars represent standard errors over 100 simulations.

5 Conclusion and Future Work

While polynomial constraints-based DAG learning algorithms achieve promising accuracy, they often suffer from gradient vanishing. We identified one important source of gradient vanishing: improper small coefficients for higher order terms, and proposed to use the geometric series based DAG constraints to escape from gradient vanishing. We further proposed an efficient algorithm that can evaluate the constraint with bounded error in $\mathcal{O}(\log k)$ complexity, where k is often far smaller than the number of nodes. By replacing the previous DAG constraints with ours, the performance of DAG learning can often be significantly improved in various settings.

A clear next step would be finding strategies to adaptively adjust the coefficients for higher terms in polynomial based constraints. In a nutshell, polynomial-based constraints may explode on candidate graphs that are far from acyclic, and also suffer from gradient vanishing problem when the graph is nearly acyclic. Fixed coefficients can not solve both problems at the same time. Another possible direction is to use the sparse properties in DAGs to make DAG learning more efficient. Since the adjacency matrix of DAG must be nilpotent, there might exist more compact representation of the adjacency matrix, such as a low-rank CANDECOMP/PARAFAC (CP) decomposition, which can potentially be used to derive an efficient algorithm for very large graphs.

References

[1] A. Al-Mohy and N. Higham. A new scaling and squaring algorithm for the matrix exponential. *SIAM Journal on Matrix Analysis and Applications*, 31, 2009.

[2] P. Bader, S. Blanes, and F. Casas. Computing the matrix exponential with an optimized taylor polynomial approximation. *Mathematics*, 7(12):1174, 2019.

[3] D. P. Bertsekas. *Constrained Optimization and Lagrange Multiplier Methods*. Academic Press, 1982.

[4] D. P. Bertsekas. *Nonlinear Programming*. Athena Scientific, 2nd edition, 1999.

[5] R. Bhattacharya, T. Nagarajan, D. Malinsky, and I. Shpitser. Differentiable causal discovery under unmeasured confounding. In *International Conference on Artificial Intelligence and Statistics*, 2021.

[6] R. H. Byrd, P. Lu, J. Nocedal, and C. Zhu. A limited memory algorithm for bound constrained optimization. *SIAM Journal on scientific computing*, 16(5):1190–1208, 1995.

[7] D. M. Chickering. Learning Bayesian networks is NP-complete. In *Learning from Data: Artificial Intelligence and Statistics V*. Springer, 1996.

[8] D. M. Chickering. Optimal structure identification with greedy search. *Journal of machine learning research*, 3(Nov):507–554, 2002.

[9] M. Chickering, D. Heckerman, and C. Meek. Large-sample learning of bayesian networks is np-hard. *Journal of Machine Learning Research*, 5, 2004.

[10] D. Colombo, M. H. Maathuis, M. Kalisch, and T. S. Richardson. Learning high-dimensional directed acyclic graphs with latent and selection variables. *The Annals of Statistics*, pages 294–321, 2012.

[11] D. Coppersmith and S. Winograd. Matrix multiplication via arithmetic progressions. *Journal of Symbolic Computation*, 9(3):251–280, 1990. ISSN 0747–7171. Computational algebraic complexity editorial.

[12] J. Cussens. Bayesian network learning with cutting planes. In *Conference on Uncertainty in Artificial Intelligence*, 2011.

[13] D. Kalainathan and O. Goudet. Causal discovery toolbox: Uncover causal relationships in python. *arXiv preprint arXiv:1903.02278*, 2019.

[14] D. E. Knuth. *The Art of Computer Programming, Volume 1: (3rd Ed.) Sorting and Searching*. 1997.

[15] M. Koivisto and K. Sood. Exact Bayesian structure discovery in Bayesian networks. *Journal of Machine Learning Research*, 5(Dec):549–573, 2004.

[16] D. Koller and N. Friedman. *Probabilistic graphical models: principles and techniques*. MIT press, 2009.

[17] S. Lachapelle, P. Brouillard, T. Deleu, and S. Lacoste-Julien. Gradient-based neural DAG learning. In *International Conference on Learning Representations*, 2020.

[18] H.-C. Lee, M. Danieletto, R. Miotto, S. T. Cherng, and J. T. Dudley. Scaling structural learning with no-bears to infer causal transcriptome networks. In *PACIFIC SYMPOSIUM ON BIOCOMPUTING 2020*, pages 391–402. World Scientific, 2019.

[19] P. L. Loh and P. Bühlmann. High-dimensional learning of linear causal networks via inverse covariance estimation. *Journal of Machine Learning Research*, 2013.

[20] I. Ng, A. Ghassami, and K. Zhang. On the role of sparsity and DAG constraints for learning linear DAGs. *Advances in Neural Information Processing Systems*, 33, 2020.

[21] I. Ng, S. Lachapelle, N. R. Ke, S. Lacoste-Julien, and K. Zhang. On the convergence of continuous constrained optimization for structure learning. In *International Conference on Artificial Intelligence and Statistics*, 2022.

[22] I. Ng, S. Zhu, Z. Fang, H. Li, Z. Chen, and J. Wang. Masked gradient-based causal structure learning. In *SIAM International Conference on Data Mining*, 2022.

[23] R. Pamfil, N. Sriwattanaworachai, S. Desai, P. Pilgerstorfer, P. Beaumont, K. Georgatzis, and B. Aragam. DYNOTEARS: Structure learning from time-series data. In *International Conference on Artificial Intelligence and Statistics*, 2020.

[24] J. Pearl. Models, reasoning and inference. *Cambridge, UK: Cambridge University Press*, 19, 2000.

[25] J. Peters and P. Bühlmann. Identifiability of Gaussian structural equation models with equal error variances. *Biometrika*, 101(1):219–228, 2013.

[26] G. Raskutti and C. Uhler. Learning directed acyclic graph models based on sparsest permutations. *Stat*, 7(1):e183, 2018.

[27] K. Sachs, O. Perez, D. Pe'er, D. A. Lauffenburger, and G. P. Nolan. Causal protein-signaling networks derived from multiparameter single-cell data. *Science*, 308(5721):523–529, 2005.

[28] A. Schrijver. *Combinatorial optimization: polyhedra and efficiency*, volume 24. Springer Science & Business Media, 2003.

[29] R. D. Shah and J. Peters. The hardness of conditional independence testing and the generalised covariance measure. *The Annals of Statistics*, 48(3):1514–1538, 2020.

[30] T. Silander and P. Myllymäki. A simple approach for finding the globally optimal Bayesian network structure. In *Conference on Uncertainty in Artificial Intelligence*, 2006.

[31] A. P. Singh and A. W. Moore. Finding optimal Bayesian networks by dynamic programming. Technical report, Carnegie Mellon University, 2005.

[32] P. Spirtes and C. Glymour. An algorithm for fast recovery of sparse causal graphs. *Social science computer review*, 9(1):62–72, 1991.

[33] P. Spirtes, C. Meek, and T. Richardson. Causal inference in the presence of latent variables and selection bias. In *Conference on Uncertainty in Artificial Intelligence*, 1995.

[34] P. Spirtes, C. N. Glymour, R. Scheines, and D. Heckerman. *Causation, prediction, and search*. MIT press, 2000.

[35] V. Strassen. Gaussian elimination is not optimal. *Numerische Mathematik*, 13:354–356, 1969.

[36] I. Tsamardinos, L. E. Brown, and C. F. Aliferis. The max-min hill-climbing bayesian network structure learning algorithm. *Machine learning*, 65(1):31–78, 2006.

[37] M. J. Vowels, N. C. Camgoz, and R. Bowden. D'ya like dags? a survey on structure learning and causal discovery. *arXiv preprint arXiv:2103.02582*, 2021.

[38] D. Wei, T. Gao, and Y. Yu. DAGs with no fears: A closer look at continuous optimization for learning bayesian networks. *arXiv preprint arXiv:2010.09133*, 2020.

[39] Y. Yu, J. Chen, T. Gao, and M. Yu. DAG-GNN: Dag structure learning with graph neural networks. In *International Conference on Machine Learning*, pages 7154–7163. PMLR, 2019.

[40] Y. Yu, T. Gao, N. Yin, and Q. Ji. DAGs with no curl: An efficient dag structure learning approach. In *Proceedings of the 38th International Conference on Machine Learning*, 2021.

[41] C. Yuan and B. Malone. Learning optimal Bayesian networks: A shortest path perspective. *Journal of Artificial Intelligence Research*, 48(1):23–65, 2013.

[42] C. Yuan, B. Malone, and X. Wu. Learning optimal Bayesian networks using A* search. In *International Joint Conference on Artificial Intelligence*, 2011.

[43] B. Zhang, C. Gaiteri, L.-G. Bodea, Z. Wang, J. McElwee, A. A. Podtelezhnikov, C. Zhang, T. Xie, L. Tran, R. Dobrin, et al. Integrated systems approach identifies genetic nodes and networks in late-onset alzheimer's disease. *Cell*, 153(3):707–720, 2013.

[44] X. Zheng, B. Aragam, P. Ravikumar, and E. P. Xing. DAGs with No Tears: Continuous optimization for structure learning. *arXiv preprint arXiv:1803.01422*, 2018.

[45] X. Zheng, C. Dan, B. Aragam, P. Ravikumar, and E. Xing. Learning sparse nonparametric dags. In *International Conference on Artificial Intelligence and Statistics*, pages 3414–3425. PMLR, 2020.

[46] R. Zhu, A. Pfadler, Z. Wu, Y. Han, X. Yang, F. Ye, Z. Qian, J. Zhou, and B. Cui. Efficient and scalable structure learning for bayesian networks: Algorithms and applications. In *2021 IEEE 37th International Conference on Data Engineering (ICDE)*, pages 2613–2624. IEEE, 2021.

Checklist

1. For all authors...
   (a) Do the main claims made in the abstract and introduction accurately reflect the paper's contributions and scope? [Yes]
   (b) Did you describe the limitations of your work? [Yes] See lines 73 and 255
   (c) Did you discuss any potential negative societal impacts of your work? [No]
   (d) Have you read the ethics review guidelines and ensured that your paper conforms to them? [Yes]
2. If you are including theoretical results...
   (a) Did you state the full set of assumptions of all theoretical results? [Yes]
   (b) Did you include complete proofs of all theoretical results? [Yes] See Appendices
3. If you ran experiments...
   (a) Did you include the code, data, and instructions needed to reproduce the main experimental results (either in the supplemental material or as a URL)? [No] We are pleased to release code on our website after the work is accepted.
   (b) Did you specify all the training details (e.g., data splits, hyperparameters, how they were chosen)? [Yes] See Appendices
   (c) Did you report error bars (e.g., with respect to the random seed after running experiments multiple times)? [Yes] See Section 4
   (d) Did you include the total amount of compute and the type of resources used (e.g., type of GPUs, internal cluster, or cloud provider)? [Yes] See Appendices
4. If you are using existing assets (e.g., code, data, models) or curating/releasing new assets...
   (a) If your work uses existing assets, did you cite the creators? [Yes]
   (b) Did you mention the license of the assets? [Yes] See Appendices

(c) Did you include any new assets either in the supplemental material or as a URL? [No]

(d) Did you discuss whether and how consent was obtained from people whose data you're using/curating? [Yes] We use public available datasets

(e) Did you discuss whether the data you are using/curating contains personally identifiable information or offensive content? [N/A]

5. If you used crowdsourcing or conducted research with human subjects...

(a) Did you include the full text of instructions given to participants and screenshots, if applicable? [N/A]

(b) Did you describe any potential participant risks, with links to Institutional Review Board (IRB) approvals, if applicable? [N/A]

(c) Did you include the estimated hourly wage paid to participants and the total amount spent on participant compensation? [N/A]

Appendices

A Proofs

A.1 Proof of Proposition 1

Proposition 1. *Let $\tilde{\mathbf{B}} \in \mathbb{R}_{\geqslant 0}^{d\times d}$ be the weighted adjacency matrix of a graph $\mathcal{G}$ with d vertices. $\mathcal{G}$ is a DAG if and only if $\tilde{\mathbf{B}}^d = \mathbf{0}$.*

Proof. Any path in a d-node DAG can not be longer than d, thus we must have $b_{ij}^{(d)} = 0$ for all i, j, which indicates for DAG we must have $\tilde{\mathbf{B}}^d = \mathbf{0}$. On the other side, a nilpotent adjacency matrix must form a DAG [38, Lemma 1]. □

A.2 Proof of Proposition 2

Proposition 2. *Let $\tilde{\mathbf{B}} \in \mathbb{R}_{\geqslant 0}^{d\times d}$ be the weighted adjacency matrix of a graph $\mathcal{G}$ with d vertices, let k be the length of longest simple path in $\mathcal{G}$, the following 3 conditions are equivalent: (1) $\mathcal{G}$ is a DAG, (2) $\tilde{\mathbf{B}}^{k+1} = 0$, and (3) $h_{trunc}^k(\tilde{\mathbf{B}}) = 0$.*

Proof. First notice that $(\tilde{\mathbf{B}}^k)_{j\ell} > 0$ if and only if there is at least a directed walk with length k from node j to node ℓ in $\mathcal{G}$. We consider the following cases:

- Case (1)→(2): Since $\mathcal{G}$ is a DAG, the diagonal entries of $\tilde{\mathbf{B}}^{k+1}$ are zero. Therefore, it suffices to consider its non-diagonal entries. For a DAG, any directed path in a DAG must be a simple path without loop. If it is not, then we can find a directed path, where a node appears twice, which means that there is a loop in the graph and it is in contradiction with the acyclic property. Thus if $\mathcal{G}$ is a DAG, there will be no path with length larger than k, and so the non-diagonal entries of $\tilde{\mathbf{B}}^{k+1}$ are zero. Combining both cases, we have $\tilde{\mathbf{B}}^{k+1} = 0$.
- Case (1)→(3): Since $\mathcal{G}$ is a DAG, the diagonal entries of $\tilde{\mathbf{B}}^i, i = 1, \ldots, d$ are zeros. Therefore, we must have $\operatorname{tr}\left(\sum_{i=1}^k \tilde{\mathbf{B}}^i\right) = 0$.
- Case (2)→(1): Since $\tilde{\mathbf{B}}^{k+1} = 0$, $\tilde{\mathbf{B}}$ is nilpotent and $\mathcal{G}$ must be acyclic.
- Case (3)→(1): It is clear that a directed graph is a DAG if and only if it does not contain simple cycle. Since $\operatorname{tr}\left(\sum_{i=1}^k \tilde{\mathbf{B}}^i\right) = 0$, all path with length smaller than or equal to k must not be a (simple) cycle. If there exists any path with length larger than k that forms a simple cycle, then there exists a simple path that is longer than k, which contradicts our assumption that k is the longest simple path. Combining both cases, $\mathcal{G}$ does not contain simple cycle and thus must be acyclic.

Here we proved that (1) and (2) are equivalent; (1) and (3) are equivalent. Thus the three conditions must be equivalent under the proposition's assumption. □

A.3 Properties of Polynomials of Matrices

In this section, we provide several properties of polynomials of matrices as basis of our following proofs.

Lemma 2. *Given $\tilde{\mathbf{B}} \in \mathbb{R}_{\geqslant 0}^{d\times d}$, assume that we have two series $[\alpha_0, \alpha_1, \ldots, \alpha_k] \in \mathbb{R}_{\geqslant 0}^{k+1}$ and $[\beta_0, \beta_1, \ldots, \beta_k] \in \mathbb{R}_{\geqslant 0}^{k+1}$, if $\forall i \in \{0, 1, \ldots k\}, \alpha_i \geqslant \beta_i$, the following inequality holds:*

$$\left\| \sum_{i=0} \alpha_i \tilde{\mathbf{B}}^i \right\|_F \geqslant \left\| \sum_{i=0} \beta_i \tilde{\mathbf{B}}^i \right\|_F, \tag{14a}$$

$$\left\| \sum_{i=0} \alpha_i \tilde{\mathbf{B}}^i \right\|_\infty \geqslant \left\| \sum_{i=0} \beta_i \tilde{\mathbf{B}}^i \right\|_\infty. \tag{14b}$$

Proof. By the fact that $\tilde{\mathbf{B}} \in \mathbb{R}_{\geqslant 0}^{d\times d}$, we must have $\forall i \in \{0, 1, \ldots, k\}, \tilde{\mathbf{B}}^i \in \mathbb{R}_{\geqslant 0}^{d\times d}$. Then by the condition that $\forall i \in \{0, 1, \ldots k\}, \alpha_i \geqslant \beta_i$, straightly we can see that each entry of $\sum_{i=0} \alpha_i \tilde{\mathbf{B}}^i$ should be no less than the corresponding entry of $\sum_{i=0} \beta_i \tilde{\mathbf{B}}^i$. Thus (14) must hold. □

A.4 Proof of Proposition 3

Proposition 3. *Given $\tilde{\mathbf{B}} \in \mathbb{R}_{\geqslant 0}^{d\times d}$, if there exists $k < d$ such that $\|\tilde{\mathbf{B}}^k\|_\infty \leqslant \epsilon < \frac{1}{(k+1)d}$, then we have*

$$0 \leqslant h_{geo}(\tilde{\mathbf{B}}) - h_{trunc}^k(\tilde{\mathbf{B}}) \leqslant d^{2+1/k} \cdot \frac{1-(d\epsilon)^{d/k-1}}{1-(d\epsilon)^{1/k}} \epsilon^{1+1/k}, \quad \textit{and}$$
$$0 \leqslant \|\nabla_{\tilde{\mathbf{B}}} h_{geo}(\tilde{\mathbf{B}}) - \nabla_{\tilde{\mathbf{B}}} h_{trunc}^k(\tilde{\mathbf{B}})\|_F \leqslant (k+1)d\epsilon \|\nabla_{\tilde{\mathbf{B}}} h_{geo}(\tilde{\mathbf{B}})\|_F.$$

Proof. Let $[\lambda_1, \lambda_2, \ldots, \lambda_d]$ be the d eigen values of $\tilde{\mathbf{B}}$. We have

$$\max_i |\lambda_i^k| \leqslant \|\tilde{\mathbf{B}}^k\|_F \leqslant d\|\tilde{\mathbf{B}}^k\|_\infty \leqslant d\epsilon, \tag{15}$$

which indicates that

$$\max |\lambda_i| \leqslant (d\epsilon)^{1/k}. \tag{16}$$

As all entries of $\tilde{\mathbf{B}}$ are non-negative, we have $\forall j > 1$

$$\mathrm{tr}\tilde{\mathbf{B}}^{k+j} = |\mathrm{tr}\tilde{\mathbf{B}}^{k+j}| = |\sum_{i=1}^d \lambda_i^{k+j}| \leqslant \sum_{i=1}^d |\lambda_i^{k+j}| \leqslant d \max_i |\lambda_i^{k+j}| = d(\max_i |\lambda_i|)^{k+j} \leqslant d^{2+j/k}\epsilon^{1+j/k},$$

which implies that

$$h_{\text{geo}}(\tilde{\mathbf{B}}) - h_{\text{trunc}}^k(\tilde{\mathbf{B}}) = \sum_{j=1}^{d-k} \mathrm{tr}\tilde{\mathbf{B}}^{k+j} \leqslant \sum_{j=1}^{d-k} d^{2+j/k}\epsilon^{1+j/k} = d^{2+1/k}\frac{1-(d\epsilon)^{d/k-1}}{1-(d\epsilon)^{1/k}}\epsilon^{1+1/k},$$

which finished the proof of the first part of the proposition. We then have the results for the second part as

$$\|\nabla_{\tilde{\mathbf{B}}}[h_{\text{geo}}(\tilde{\mathbf{B}}) - h^k_{\text{trunc}}(\tilde{\mathbf{B}})]\|_F = \underbrace{\left\|\sum_{j=1}^{d-k}(k+j)\,\mathbf{B}^{k+j-1}\right\|_F \leqslant \left\|\sum_{j=1}^{d-k}(kj+j)\,\mathbf{B}^{k+j-1}\right\|_F}_{kj+j\geqslant k+j \text{ for } j=1,2,\ldots d-k, \text{then by Lemma 2}}$$

$$= \underbrace{(k+1)\left\|\tilde{\mathbf{B}}^k\sum_{j=1}^{d-k} j\tilde{\mathbf{B}}^{j-1}\right\|_F \leqslant (k+1)\|\tilde{\mathbf{B}}^k\|_F\left\|\sum_{j=1}^{d-k} j\tilde{\mathbf{B}}^{j-1}\right\|_F}_{\text{Submultiplicative of Frobenius norm}}$$

$$= \underbrace{(k+1)\|\tilde{\mathbf{B}}^k\|_F\left\|\sum_{j=1}^{d-k} j\tilde{\mathbf{B}}^{j-1} + \sum_{j=d-k+1}^{d} 0\times\tilde{\mathbf{B}}^{j-1}\right\|_F \leqslant (k+1)\|\tilde{\mathbf{B}}^k\|_F\left\|\sum_{j=1}^{d} j\tilde{\mathbf{B}}^{j-1}\right\|_F}_{\text{From Lemma 2}}$$

$$\leqslant \underbrace{(k+1)d\epsilon\left\|\sum_{j=1}^{d} j\tilde{\mathbf{B}}^{j-1}\right\|_F}_{\text{By Eq.(15)}} = (k+1)d\epsilon\|\nabla_{\tilde{\mathbf{B}}}h_{\text{geo}}(\tilde{\mathbf{B}})\|_F.$$

□

A.5 Proof of Proposition 4

Proposition 4. *Given any $d\times d$ real matrix $\tilde{\mathbf{B}}$, let $f_i(\tilde{\mathbf{B}}) = \tilde{\mathbf{B}}+\tilde{\mathbf{B}}^2+\cdots+\tilde{\mathbf{B}}^i$ and $h_i(\tilde{\mathbf{B}}) = \mathrm{tr}(f_i(\tilde{\mathbf{B}}))$, we have the following recurrence relations:*

$$\begin{aligned} f_{i+j}(\tilde{\mathbf{B}}) =& f_i(\tilde{\mathbf{B}}) + \tilde{\mathbf{B}}^i f_j(\tilde{\mathbf{B}}),\\ \nabla_{\tilde{\mathbf{B}}}h_{i+j}(\tilde{\mathbf{B}}) =& \nabla_{\tilde{\mathbf{B}}}h_i(\tilde{\mathbf{B}}) + (\tilde{\mathbf{B}}^i)^\top\nabla_{\tilde{\mathbf{B}}}h_j(\tilde{\mathbf{B}}) + if_j(\tilde{\mathbf{B}})^\top(\tilde{\mathbf{B}}^{i-1})^\top. \end{aligned}$$

Proof. Substituting $i+j$ for i in the definition of $f_i(\tilde{\mathbf{B}})$, we have

$$\begin{aligned} f_{i+j}(\tilde{\mathbf{B}}) &= \tilde{\mathbf{B}} + \tilde{\mathbf{B}}^2 + \cdots + \tilde{\mathbf{B}}^i + \tilde{\mathbf{B}}^{i+1} + \tilde{\mathbf{B}}^{i+2} + \cdots + \tilde{\mathbf{B}}^{i+j}\\ &= (\tilde{\mathbf{B}} + \tilde{\mathbf{B}}^2 + \cdots + \tilde{\mathbf{B}}^i) + (\tilde{\mathbf{B}}^{i+1} + \tilde{\mathbf{B}}^{i+1} + \tilde{\mathbf{B}}^{i+2} + \cdots + \tilde{\mathbf{B}}^{i+j})\\ &= f_i(\tilde{\mathbf{B}}) + \tilde{\mathbf{B}}^i(\tilde{\mathbf{B}} + \tilde{\mathbf{B}}^2 + \cdots + \tilde{\mathbf{B}}^j) = f_i(\tilde{\mathbf{B}}) + \tilde{\mathbf{B}}^i f_j(\tilde{\mathbf{B}}). \end{aligned}$$

Similarly, to establish the recurrence relation for $\nabla h_{i+j}(\tilde{\mathbf{B}})$, we have

$$\begin{aligned} \nabla h_{i+j}(\tilde{\mathbf{B}}) &= \nabla\mathrm{tr}(f_{i+j}(\tilde{\mathbf{B}}))\\ &= \nabla\mathrm{tr}(f_i(\tilde{\mathbf{B}})) + \nabla\mathrm{tr}(\tilde{\mathbf{B}}^i f_j(\tilde{\mathbf{B}}))\\ &= \nabla h_i(\tilde{\mathbf{B}}) + \nabla\mathrm{tr}(\tilde{\mathbf{B}}^i f_j(\tilde{\mathbf{B}}))\\ &= \nabla h_i(\tilde{\mathbf{B}}) + (\tilde{\mathbf{B}}^i)^\top\nabla\mathrm{tr}(f_j(\tilde{\mathbf{B}})) + f_j(\tilde{\mathbf{B}})^\top\nabla\mathrm{tr}(\tilde{\mathbf{B}}^i)\\ &= \nabla h_i(\tilde{\mathbf{B}}) + (\tilde{\mathbf{B}}^i)^\top\nabla h_j(\tilde{\mathbf{B}}) + if_j(\tilde{\mathbf{B}})^\top(\tilde{\mathbf{B}}^{i-1})^\top \end{aligned}$$

where the fourth equality follows from the product rule. □

A.6 Proof of Proposition 5

Proposition 5. *Given $\tilde{\mathbf{B}} \in \mathbb{R}^{d\times d}_{\geqslant 0}$, if for some k, $\|\tilde{\mathbf{B}}^k\|_\infty \leqslant \epsilon < 1/d$, then*

$$\left\|(\mathbb{I}-\tilde{\mathbf{B}})^{-1} - \sum_{i=0}^{k}\tilde{\mathbf{B}}^k\right\|_F \leqslant d\epsilon\left\|(\mathbb{I}-\tilde{\mathbf{B}})^{-1}\right\|_F.$$

Proof. Under the assumption of the proposition, the spectral radius of $\tilde{\mathbf{B}}$ is upper bounded by $(d\epsilon)^{1/k}$ with similar reasoning in (16), and therefore we can write $(\mathbb{I}-\tilde{\mathbf{B}})^{-1}=\sum_{j=0}^{\infty}\tilde{\mathbf{B}}^{j}$. Thus we have

$$\begin{aligned}\left\|(\mathbb{I}-\tilde{\mathbf{B}})^{-1}-\sum_{i=0}^{k}\tilde{\mathbf{B}}^{k}\right\|_F&=\left\|\sum_{j=1}^{\infty}\tilde{\mathbf{B}}^{k+j}\right\|_F=\left\|\tilde{\mathbf{B}}^{k}\sum_{j=1}^{\infty}\tilde{\mathbf{B}}^{j}\right\|_F\\ \leqslant\|\tilde{\mathbf{B}}^{k}\|_F\left\|\sum_{j=0}^{\infty}\tilde{\mathbf{B}}^{j}\right\|_F&\leqslant d\|\tilde{\mathbf{B}}^{k}\|_\infty\left\|(\mathbb{I}-\tilde{\mathbf{B}})^{-1}\right\|_F=d\epsilon\left\|(\mathbb{I}-\tilde{\mathbf{B}})^{-1}\right\|_F.\end{aligned}$$

□

B Fast Matrix Power Iteration

B.1 Derivation of the Algorithm

Before proceeding to Algorithm 2, we first give a proof of Corollary 1 as follows.

$$\begin{aligned}f_{2i}(\tilde{\mathbf{B}})&=\tilde{\mathbf{B}}+\tilde{\mathbf{B}}^{2}+\ldots+\tilde{\mathbf{B}}^{i}+\tilde{\mathbf{B}}^{i+1}+\tilde{\mathbf{B}}^{i+2}+\ldots+\tilde{\mathbf{B}}^{2i}\\&=f_i(\tilde{\mathbf{B}})+\tilde{\mathbf{B}}^{i}f_i(\tilde{\mathbf{B}})=\left[\mathbb{I}+\tilde{\mathbf{B}}^{i}\right]f_i(\tilde{\mathbf{B}})\end{aligned}$$

$$\begin{aligned}\nabla h_{2i}(\tilde{\mathbf{B}})=&\nabla\mathrm{tr}\left[f_i(\tilde{\mathbf{B}})\right]+\nabla\mathrm{tr}\left[\tilde{\mathbf{B}}^{i}f_i(\tilde{\mathbf{B}})\right]\\=&\nabla\mathrm{tr}\left[f_i(\tilde{\mathbf{B}})\right]+(\tilde{\mathbf{B}}^{i})^{\top}\nabla\mathrm{tr}\left[f_i(\tilde{\mathbf{B}})\right]+\left[f_i(\tilde{\mathbf{B}})\right]^{\top}\nabla\mathrm{tr}\left[\tilde{\mathbf{B}}^{i}\right]\\=&\left[\mathbb{I}+\tilde{\mathbf{B}}^{i}\right]^{\top}\nabla\mathrm{tr}\left[f_i(\tilde{\mathbf{B}})\right]+i\left[f_i(\tilde{\mathbf{B}})\right]^{\top}\left[\tilde{\mathbf{B}}^{i-1}\right]^{\top}\\=&\left[\mathbb{I}+\tilde{\mathbf{B}}^{i}\right]^{\top}\nabla\mathrm{tr}\left[f_i(\tilde{\mathbf{B}})\right]+i\underbrace{\left[f_{2i}(\tilde{\mathbf{B}})-f_i(\tilde{\mathbf{B}})+\tilde{\mathbf{B}}^{i}-\tilde{\mathbf{B}}^{2i}\right]^{\top}}_{=\left[f_i(\tilde{\mathbf{B}})\right]^{\top}\left[\tilde{\mathbf{B}}^{i-1}\right]^{\top}}\end{aligned}$$

To lighten the notation, hereafter we use $\nabla h_i(\tilde{\mathbf{B}})$ to indicate to $\nabla_{\tilde{\mathbf{B}}}h_i(\tilde{\mathbf{B}})$. The full procedure of the proposed fast matrix power iteration algorithm is described in Algorithm 2, which computes both the DAG constraint term and its gradient. The algorithm requires $\mathcal{O}(\log k)$ matrix multiplications and $\mathcal{O}(d^2)$ storage, and we provide an example implementation in Figure 5.

```python
import numpy as np


def h_fast_tmpi(B, eps=1e-6):
    d = B.shape[0]
    global old_g
    global old_B
    global sec_g
    if old_g is None:
        old_g = np.zeros_like(B)
        old_B = np.zeros_like(B)
        sec_g = np.zeros_like(B)
    if old_g.shape[0] != d:
        old_g = np.zeros_like(B)
        old_B = np.zeros_like(B)
        sec_g = np.zeros_like(B)
    _B = np.copy(B)
    _g = np.copy(B)
    _grad = np.eye(d)

    j = 1
    while j <= d:
        np.copyto(old_B, _B)
        np.copyto(old_g, _g)
        np.matmul(_B, _g, out=_g)
        np.add(old_g, _g, out=_g)

        np.copyto(sec_g, _grad)
        np.matmul(_B.T, _grad, out=_grad)
        np.matmul(_B, _B, out=_B)
        np.add(_grad, sec_g, out=_grad)
        np.copyto(sec_g, _g)
        sec_g -= old_g
        sec_g += old_B
        sec_g -= _B
        sec_g *= j

        _grad += sec_g.T

        if np.max(np.abs(_B)) < eps:
            break
        j *= 2

    return np.trace(_g), _grad
```

Figure 5: An example implementation of Algorithm 2.

B.2 Comparison of time complexity of different DAG constraints

The time complexity for computing the proposed DAG constraints, along with the existing ones, is provided in Table 2. Note that the complexity is described in terms of matrix multiplications, whose efficient algorithms have received much attention in the field of numerical linear algebra in the past decades. Coppersmith–Winograd [11] algorithm and Strassen algorithm [35] are widely used and require $\mathcal{O}(d^{2.376})$ and $\mathcal{O}(d^{2.807})$ operations, respectively.

C Additional Experiment Results

C.1 Additional results on ER graphs

The False Discovery Rate (FDR), True Positive Rate (TPR) and False Positive Rate (FPR) are shown in provided in this section, and our TMPI based algorithm often achieves best performance in all these criteria.

Table 2: Complexity of different DAG constraints terms and their gradients in terms of matrix multiplications.

DAG constraint term (and its gradient)	Complexity
Matrix exponential [44][i]	$\mathcal{O}(d)$
Binomial [39] [ii]	$\mathcal{O}(\log d)$
Polynomial [38]	$\mathcal{O}(d)$
NOBEARS [18]	$\mathcal{O}(1)$
Single term	$\mathcal{O}(\log d)$
Geometric	$\mathcal{O}(d)$
Fast geometric	$\mathcal{O}(\log d)$
TMPI	$\mathcal{O}(k)$
Fast TMPI	$\mathcal{O}(\log k)$

[i] More precisely, the complexity of matrix exponential depends on the desired accuracy of the computation, for which a wide variety of algorithms are available [1, 2]. Here we use a fixed complexity since the first d terms of the Taylor expansion are sufficient to form a DAG constraint. [ii] Based on exponentiation by squaring.

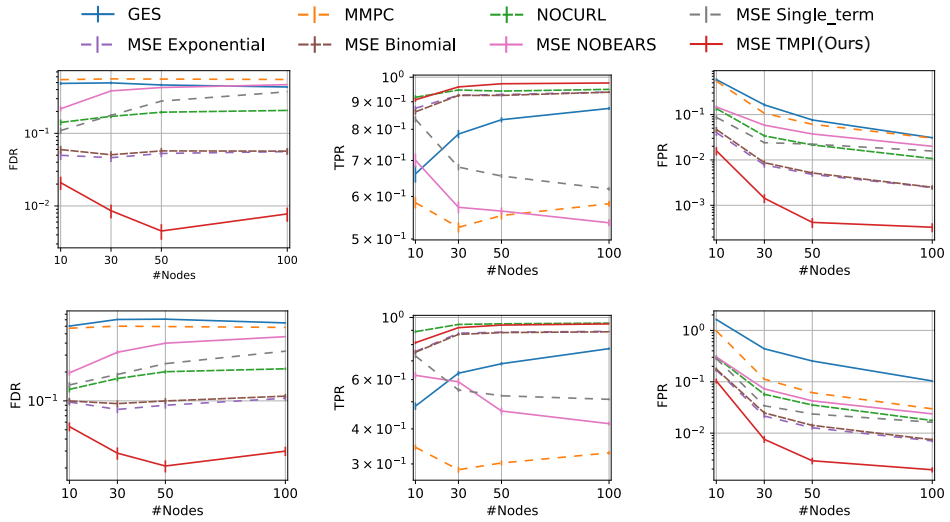

Figure 6: False Discovery Rate (FDR, lower is better), True Positive Rate (TPR, higher is better) and False Positive Rate (FPR, lower is better) of MSE based algorithms on ER2 (top) and ER3 (bottom) graphs.

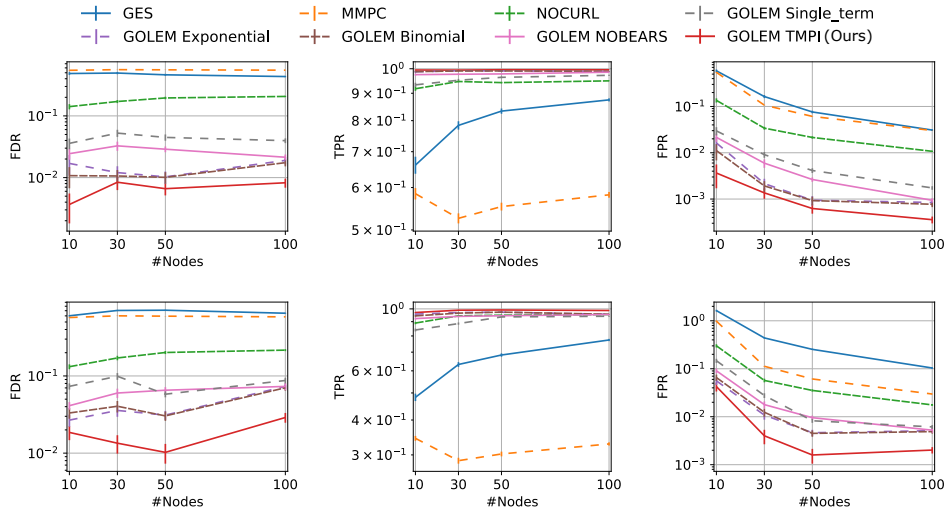

Figure 7: False Discovery Rate (FDR, lower is better), True Positive Rate (TPR, higher is better) and False Positive Rate (FPR, lower is better) of likelihood loss based algorithms on ER2 (top) and ER3 (bottom) graphs.

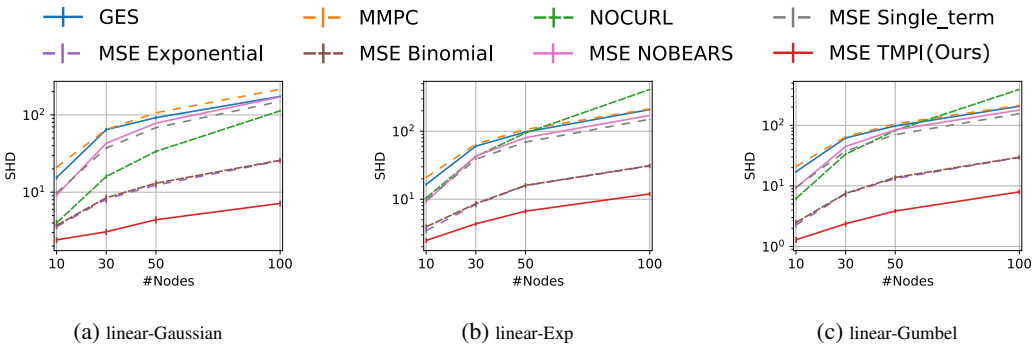

(a) linear-Gaussian (b) linear-Exp (c) linear-Gumbel

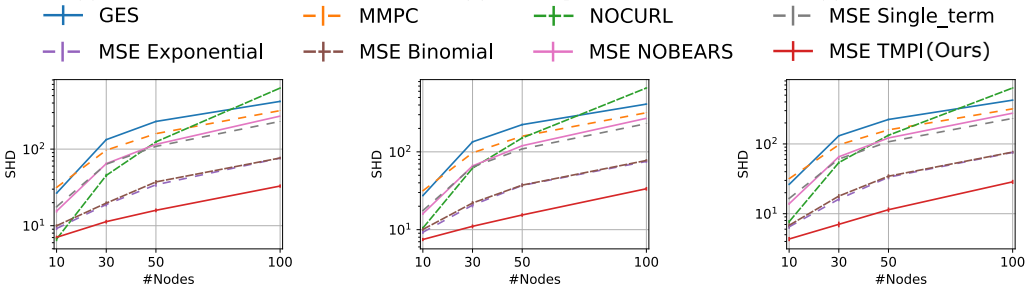

(d) linear-Gaussian (e) linear-Exp (f) linear-Gumbel

Figure 9: Results with 200 samples on ER2 (top) and ER3 (bottom) graphs.

C.2 Additonal results on SF graphs

We have conducted additional experiments for the *Scale-Free* graph model and the results is shown in Figures 8, where we can see that with different graph structures our algorithm consistently gets better results.

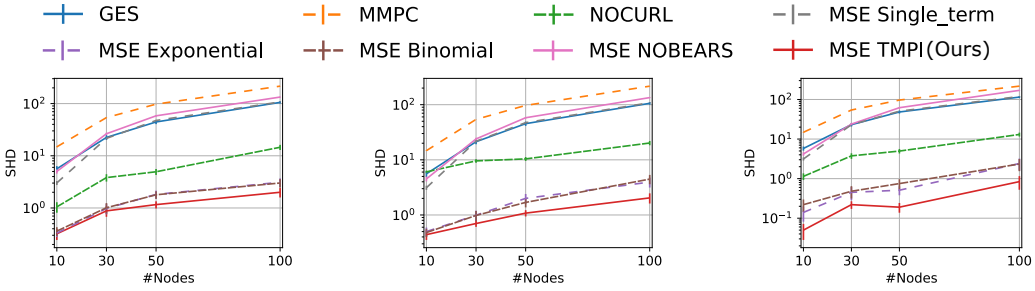

(a) linear-Gaussian (b) linear-Exp (c) linear-Gumbel

Figure 8: SHD of different algorithms on SF2 graphs.

C.3 Experimental results with less samples

We also conducted an experiment with less observed samples (200 samples) on the linear Gaussian synthetic data, and the results are shown in Figure 9, where our algorithm outperforms all others in most of the cases.

C.4 Experiments on Large Scale Graph

We have conducted experiments on ER2 graph with 500 nodes with Gaussian noises. For these kind of graphs, the GOLEM algorithm is known to perform well [20]. Thus we combine the GOLEM algorithm with different DAG constraints, where for all DAG constraints, the parameters λ_1 and λ_2 for GOLEM algorithm are set to $2e-2$ and 5.0, and the number of iterations is set to 70000. The

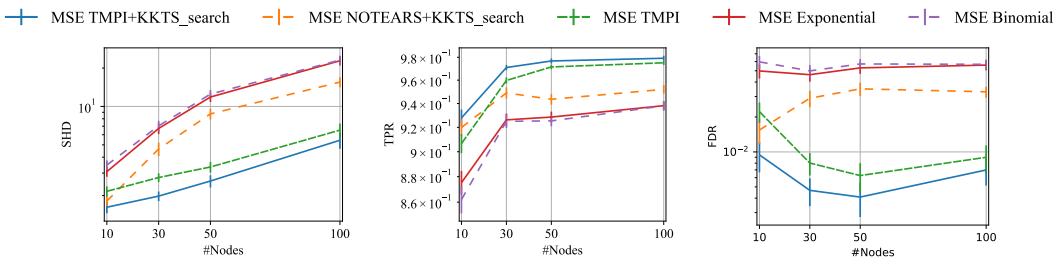

Figure 10: Comparison with KKT based local search strategy [38] on ER2 graph with linear Gaussian SEMs. The results are averaged from 100 instances. The NOFEARS method (NOTEARS+KKTS search) achieves better performance the original NOTEARS (MSE Exponential), but it still performance worse than our TMPI in most cases. The method that combines our TMPI and local search (TMPI+KKTS search) achieves best performance.

results are shown in Table 3 and our algorithm achieves the best SHD and fastest running time. The running time are measured on a server with V100 GPU.

	GOLEM + Exponetial	GOLEM + Binomial	GOLEM + TMPI
SHD ↓	45.20±6.44	46.75±7.41	**14.45±2.27**
Running Time(s) ↓	882.22±1.08	795.24±1.24	**670.26±0.76**

Table 3: Experiments on 500-node ER2 graph with Gaussian noise. Best results are in bold. All results are averaged from 20 different graph, along with the standard error.

C.5 Comparison with NOFEARS

Wei et al. [38] and Ng et al. [21] mentioned that the operation $\mathbf{B} \odot \mathbf{B}$ is one source of gradient vanishing. Based on the observation, Wei et al. [38] proposed a KKT condition based local search strategy (named NOFEARS) to avoid gradient vanishing caused by $\mathbf{B} \odot \mathbf{B}$. As shown by Wei et al. [38], to attain best performance the NOFEARS method is applied as a post-processing procedure for NOTEARS[44]. Our method identified a different source of gradient vanishing caused by the small coefficients for higher order terms in DAG constraints. Thus our work is in parallel with previous work [21, 38], and the local search strategy by Wei et al. [38] can be combined with our technique. We compared the performance of our algorithm and NOFEARS [38] in Figure 10, where our method outperforms the original NOFEARS (NOTEARS+KKTS search) in most cases. The method that combines our method and NOFEARS attains the best performance (i.e., lowest SHD and False Detection Rate (FDR), highest True Positive Rate (TPR)).

C.6 Experiments on ER6 graphs

We have conducted a simple experiment on ER6 graphs to compare the performance of different polynomial constraints on ER6 graphs (where the expected degree of node is 12). The dataset generating procedure for ER6 graph is the same as Section 4, but the number of samples n is set to 5000. The result is shown in Figure 11, where our TMPI method achieves best performance (i.e., lowest SHD and False Detection Rate (FDR), highest True Positive Rate (TPR)).

D Additional Ablation Study

We also added an ablation study to show the numeric difference between different k for our DAG constraints (Shown in Figure 12). We can see that typically the error of our truncated DAG constraints against the geometric series based DAG constraint drops exponentially as k increases. Furthermore, it is quite often this error would exceed the machine precision. Thus in our TMPI algorithm, the k is often not large, and thus the TMPI algorithm is usually faster than both the geometric and fast geometric

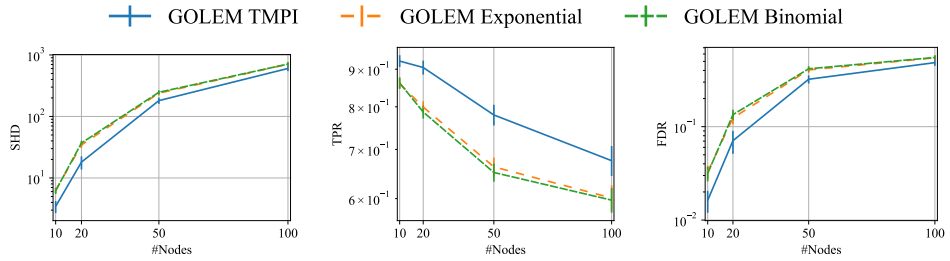

Figure 11: Comparison of different polynomial based DAG constraints on ER6 graphs. All results are averaged from 20 different graphs.

method, and our $\mathcal{O}(\log k)$ fast TMPI algorithm futher accelerated the procedure and its speed is fastest.

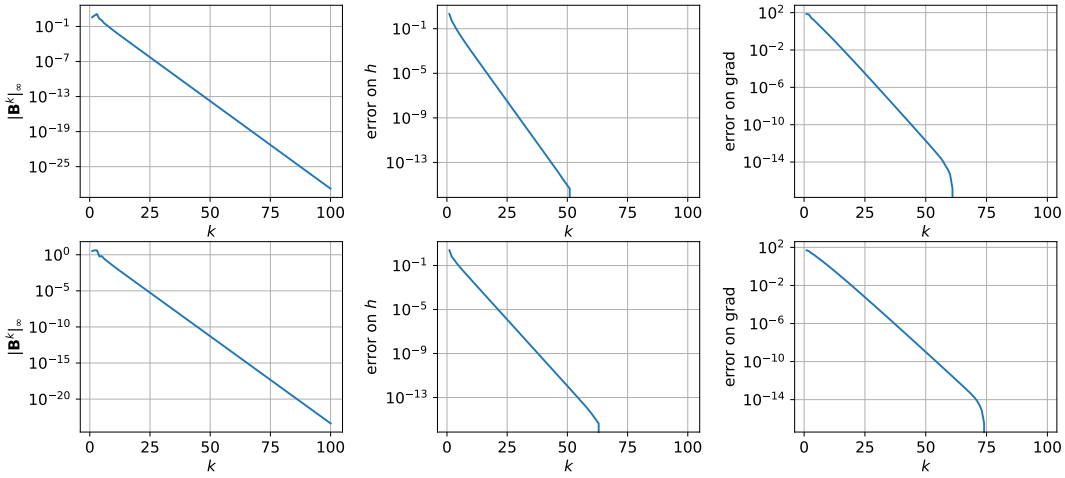

Figure 12: Typical curve of $\|\tilde{\mathbf{B}}^k\|_\infty$, error of h^k_{trunc} against h_{geo}, and error of $\nabla h^k_{\text{trunc}}$ against ∇h_{geo} (in terms of infinity norm). The left three curves are from the ER2 and the right three are from ER3.